物理探鉱 第34巻 第5号（昭和56年10月）
BUTSURI-TANKŌ (GEOPHYSICAL EXPLORATION) VOL. 34, NO. 5 (1981)

Reduction of Magnetic Anomalies to and from an Arbitrary Surface

Tadashi NAKATSUKA*

1. Introduction

In quantitative analysis and interpretation of magnetic anomalies, it is essential to reduce the anomaly observed on an irregular surface into a constant level one. This is because most of quantitative analyses in use of various filtering or automatic modeling are usable for coplaner mesh data. The effect of the elevation of observation point can be devided into two parts; one is the decrease or increase of normal field strength, and the other is the effect of varying distance from the anomalous body. As the former can be calculated from the appropreate regional (or global) normal field model, the latter is the subject to consider.

Many authers studied the method to reduce magnetic anomalies observed on an irregular surface to another surface. (DAMPNEY (1969), HENDERSON and CORDELL (1971), SYBERG (1972), etc.) Earlier studies of this kind are based on the harmonic analysis or matrix inversion, and involve some approximations or some limitations. Sammerizing those studies, BHATTACHARYYA and CHAN (1977) suggested a new reduction procedure in which observed field is converted into a surface distribution of magnetic moment normal to the surface as an equivalent source. The superior idea in this procedure is to use the surface of equivalent source identical with the observation surface, and this brings us an intense advantage for solving the problem easily.

However, BHATTACHARYYA and CHAN (1977) made a slight mistake in their theoretical consideration, and consequently, their method can be applied only under the approximation that the observation surface does not contain so high topographic relief. Succeeding their superior idea, this paper gives an improved reduction procedure which requires no such topological assumption of observation surface.

Manuscript received March 2, 1981

* Geological Survey of Japan, 1-3 Higashi-1, Yatabe-machi, Tsukuba-gun, Ibaraki-ken, 305 Japan.

2. Theoretical Consideration

Let us consider a distribution of magnetic dipole moment on an infinite (or closed) surface S. Here we let $\boldsymbol{J}$ be the magnetic moment per unit area at a point (α, β, γ) on this surface S. Then the potential U at a point $P(x, y, z)$ outside this surface is given by

$$U=\int_S (\boldsymbol{J}\cdot\boldsymbol{R}/R^3)ds, \tag{1}$$

where $R=|\boldsymbol{R}|$,

$$\boldsymbol{R}=\boldsymbol{i}(x-\alpha)+\boldsymbol{j}(y-\beta)+\boldsymbol{k}(z-\gamma),$$

and $\boldsymbol{i}$, $\boldsymbol{j}$, and $\boldsymbol{k}$ are the unit vectors along x-, y-, and z-axis, respectively. Here we use a cartesian coordinate system with z-axis pointing vertically downward. Total field anomaly T at the point $P(x, y, z)$ is then given by

$$T=-\boldsymbol{t}\cdot\nabla U, \tag{2}$$

where $\nabla=\boldsymbol{i}\dfrac{\partial}{\partial x}+\boldsymbol{j}\dfrac{\partial}{\partial y}+\boldsymbol{k}\dfrac{\partial}{\partial z}$,

and $\boldsymbol{t}$ is the unit vector in the direction of normal field. Here we introduce a unit vector $\boldsymbol{p}$ in the direction of dipole moment, and let

$$\boldsymbol{J}=J\boldsymbol{p}, \tag{3}$$

$$K=\boldsymbol{p}\cdot\boldsymbol{R}/R^3. \tag{4}$$

Combining (3), (4) and (1), we obtain

$$U=\int_S (JK)ds, \tag{5}$$

and, from (2) and (5), we have

$$T=-\int_S \boldsymbol{t}\cdot\boldsymbol{\nabla}(JK)ds$$
$$=-\int_S J(\boldsymbol{t}\cdot\boldsymbol{\nabla})Kds. \qquad (6)$$

Since the potential U is a function of (x, y, z),

$$\boldsymbol{t}\cdot\boldsymbol{\nabla}_0 U=0, \qquad (7)$$

where $\boldsymbol{\nabla}_0=\boldsymbol{i}\frac{\partial}{\partial\alpha}+\boldsymbol{j}\frac{\partial}{\partial\beta}+\boldsymbol{k}\frac{\partial}{\partial\gamma}$.

Substituting the expression (5) for U into (7), we have

$$\int_S J(\boldsymbol{t}\cdot\boldsymbol{\nabla}_0)Kds+\int_S K(\boldsymbol{t}\cdot\boldsymbol{\nabla}_0)Jds=0. \qquad (8)$$

Therefore, from (6) and (8), we obtain the following relation;

$$T=-\int_S \mu Kds-\int_S J\{\boldsymbol{t}\cdot(\boldsymbol{\nabla}+\boldsymbol{\nabla}_0)K\}ds, \qquad (9)$$

where $\mu=(\boldsymbol{t}\cdot\boldsymbol{\nabla}_0)J. \qquad (10)$

Here, K is a function of $\boldsymbol{p}$ and $\boldsymbol{R}$, as defined by (4). So, from the definitions of $\boldsymbol{\nabla}$, $\boldsymbol{\nabla}_0$ and $\boldsymbol{R}$, we can easily derive next equation, if $\boldsymbol{p}$ is a constant vector.

$$(\boldsymbol{\nabla}+\boldsymbol{\nabla}_0)K=0. \qquad (11)$$

If then, substitution of (11) into (9) gives

$$T=-\int_S \mu Kds. \qquad (12)$$

Now, as the model used by BHATTACHARYYA and CHAN (1977) is a distribution of magnetic moment perpendicular to the surface S, unit vector $\boldsymbol{p}$ in the direction of magnetic moment is dependent on the shape of the surface S, and not a constant vector. Nevertheless, they happened to apply the equation (11) into (9), and derived the equation (12). This implies that they have effectively introduced an approximation that the surface S is not so irregular.

Here, we can consider a distribution of vertical magnetic moment on the surface S, to avoid such approximation. Then, as the unit vector $\boldsymbol{p}$ is constant ($\boldsymbol{p}=\boldsymbol{k}$), (11) and (12) are derived reasonably. Also,

$$K=(z-\gamma)/R^3 \qquad (13)$$

Hereafter we deal with the distribution of vertical magnetic moment.

If the point $P(x, y, z)$ approaches a point $Q(\alpha', \beta', \gamma')$ on the surface S along a normal to the surface, we can derive the limiting form of (12) as follows:

$$T_S(\alpha', \beta', \gamma')=2\pi n'\mu(\alpha', \beta', \gamma')-\int_{S'}\mu Kds, \qquad (14)$$

where S' is the surface S without the point $Q(\alpha', \beta', \gamma')$, and n' is the z-component of the unit vector $\boldsymbol{n}$ normal to the surface S at Q. The detailed derivation of (14) is presented in Appendix A.

Now, we regard the surface S as an observation surface. Then, T_S denotes the observed total field anomaly, and it is related by the equation (14) to the gradient (μ) of dipolar distribution in the direction of normal field. Furthermore, the equation (12) gives us the formula of calculating anomaly field at an arbitrary position. That is, we can easily get the reduced anomaly field on an arbitrary surface, if we solve the integral equation (14) with respect to unknown value μ.

Equation (14) can be solved, as was described by BHATTACHARYYA and CHAN (1977), using an iteration as follows.

Transformation of (14) yields next expression:

$$\mu(\alpha', \beta', \gamma')=\frac{T_S(\alpha', \beta', \gamma')}{2\pi n'}+\frac{1}{2\pi n'}\int_{S'}\frac{\mu(\alpha, \beta, \gamma)(\gamma'-\gamma)}{R^3 n(\alpha, \beta, \gamma)}d\alpha d\beta, \qquad (15)$$

where $n(\alpha, \beta, \gamma)$ is the z-component of the unit vector normal to the surface S. Substituting i-th order approximation of μ into the right-hand side of (15), we obtain the $(i+1)$-th order approximation which is to be substituted into the right-hand side of (15) in the next step. Here, $(T_S/2\pi n')$ is used as the 0-th order approximation of μ. This iteration is continued till the approximation of μ converge enough.

3. Model Examples and Discussion

In order to demonstrate the improvement of reduction result, three model examples are presented bellow.

Case 1 represented in Fig.1a–d is the same example as was shown by BHATTACHARYYA and CHAN (1977). The observation surface is

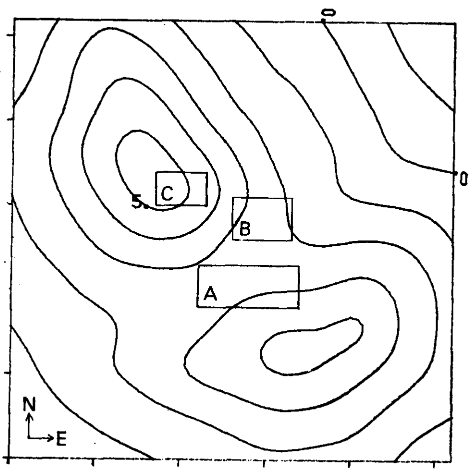

Fig. 1a Observation surface and horizontal section of magnetic bodies for Case 1.

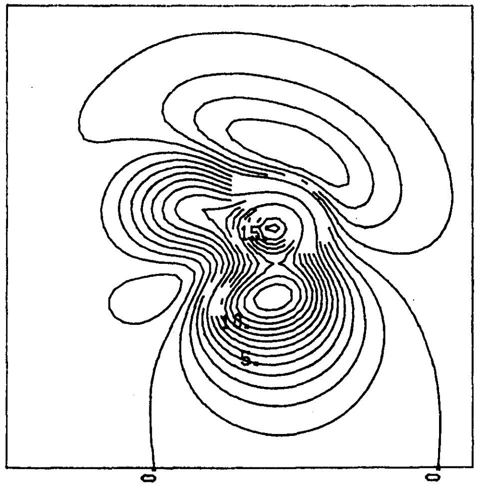

Fig. 1b Total field anomaly on the observation surface for Case 1. This is the source data of reduction processes.

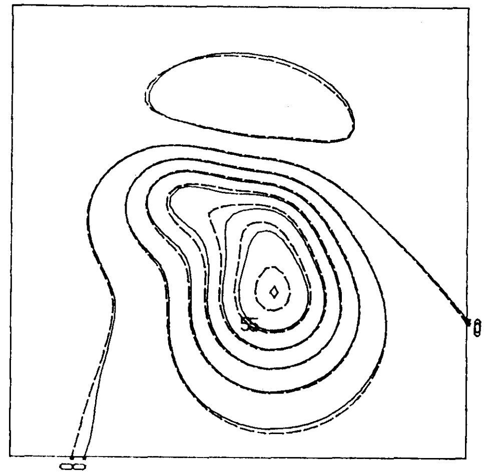

Fig. 1c Reduced total field anomaly (solid lines) and real anomaly (broken lines) for Case 1 on a horizontal plane at the height of 7 units. Reduction was made after BHATTACHARYYA and CHAN (1977).

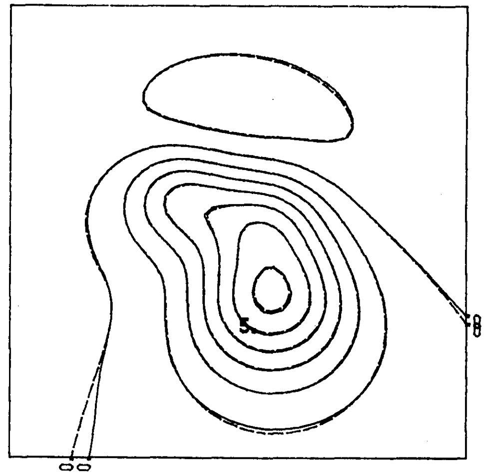

Fig. 1d Reduced total field anomaly (solid lines) and real anomaly (broken lines) for Case 1 on a horizontal plane at the height of 7 units. Reduction was made after this paper.

expressed by topographic contour-lines in Fig. 1a, and the horizontal section of model structure of magnetic bodies is superimposed. Other model parameters are listed in Table 1. Full screen of each illustration is covered with (53×53) square-mesh points, at which the calculation was carried out. Mesh size is one in arbitrary unit common with depth parameters and heights. Fig.1b indicates the observed magnetic anomaly generated by the model structure. This anomaly field, which was calculated theoretically (refer to Appendix B), is the input data for reduction process. Two reduction procedures are applied to this model to calculate the anomaly field on the plane at the height of 7 units ($z=-7$); one is the method just described by BHATTACHARYYA and CHAN (1977), and the other is the modified method described in the previous section. Results of both methods are shown in Fig.1c

Table 1　Model parameters

Block Model	A	B	C	D	E	F	G	H	J	K
Depth to the Top	2	3	1	5	3	3	4	2	1	5
Depth to the Bottom	7	7	7	15	15	15	10	10	5	10
Magnetization	20	40	20	10	10	10	25	15	20	15
Inclination	30°	72°	60°	60°	65°	65°	60°	80°	-50°	40°
Declination	45°W	5°E	10°E	0°	20°E	20°E	10°E	60°E	100°W	0°
Normal Field Direction	Inclination : 65° , Declination : 20°E									

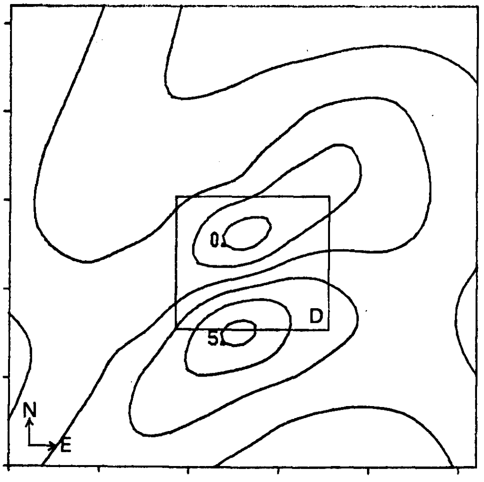

Fig. 2a　Same as Fig. 1a for Case 2.

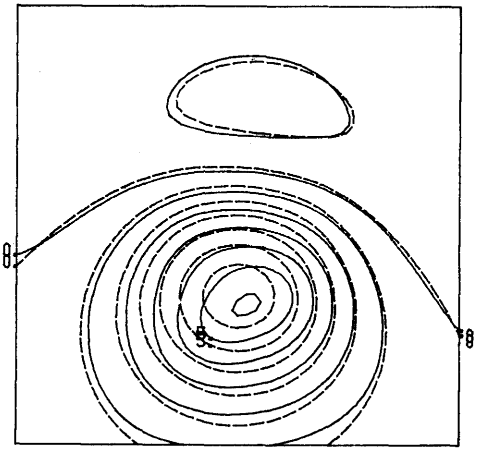

Fig. 2c　Same as Fig. 1c for Case 2.

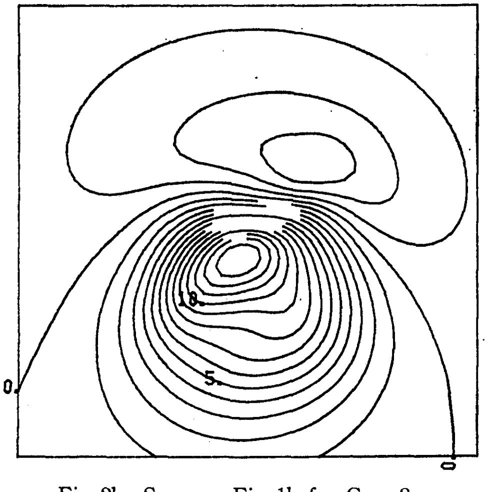

Fig. 2b　Same as Fig. 1b for Case 2.

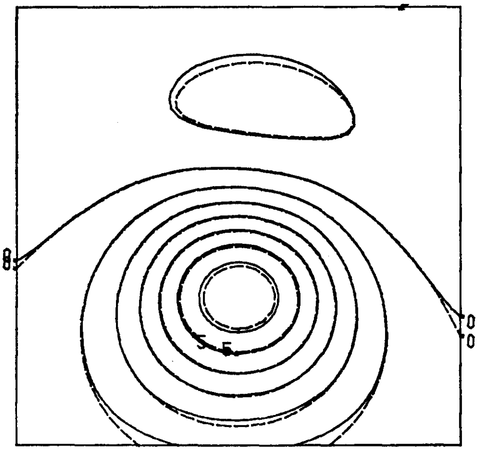

Fig. 2d　Same as Fig. 1d for Case 2.

and Fig.1d, respectively, on which real anomaly calculated directly from the model structure is superposed as a convenience of comparison.

There are another two cases illustrated in Fig.2a–d (Case 2) and Fig.3a–d (Case 3), each suffix a–d of which corresponds to the same meaning as Fig.1a–d. Throughout Case 1–3,

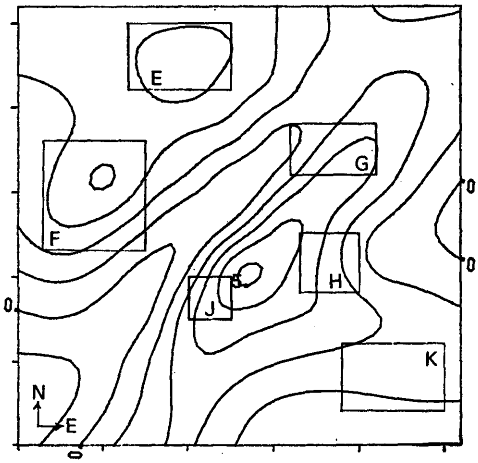

Fig. 3a Same as Fig. 1a for Case 3.

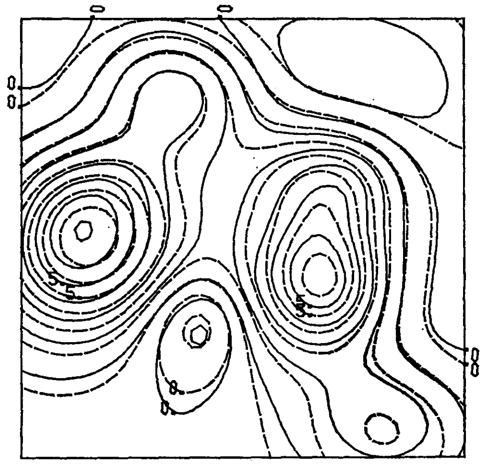

Fig. 3c Same as Fig. 1c for Case 3.

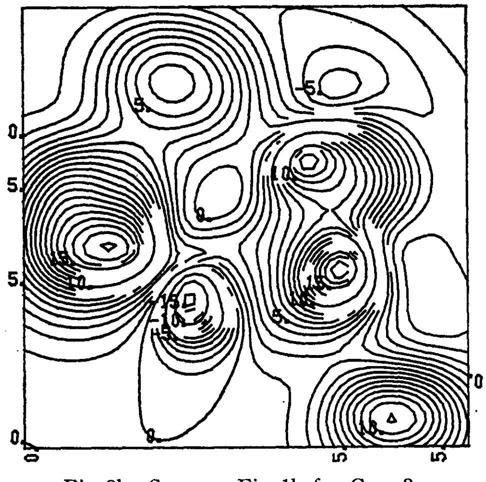

Fig. 3b Same as Fig. 1b for Case 3.

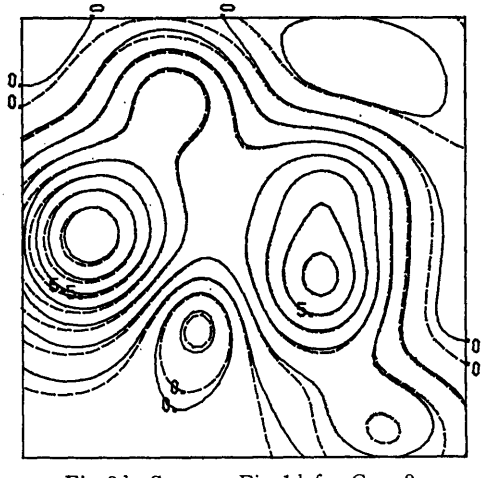

Fig. 3d Same as Fig. 1d for Case 3.

numerical integration was executed over the window of (41×41) squares area as was suggested by BHATTACHARYYA and CHAN (1977).

In Case 1, the observation surface is less distorted and not so steep; maximum points are considerably separated each other, and the slope at the steepest point is about 18°. In consequence of such situation, there is only a slight difference between the results of two methods.

On the contrary, we can see a distinct difference in Case 2. This indicates that the assumption mentioned in the previous section is not valid for this example. The maximum slope of the observation surface is about 38° in this case, and is quite a probable value in the ground magnetic survey.

Also in Case 3, the advantage of our method is clear in the central part of the illustration. However, at the edge-side in Fig.3d, there is a considerable discrepancy between reduced anomaly and real anomaly.

In the theoretical formulation, we dealt the observation surface S as an infinite (or closed) surface. But, in practical problem, we scissored the range of integration into a rectangular screen. Here is an important assumption that the contribution of the equivalent source outside this screen is small enough. In former two cases the magetic bodies are concentrated in the center of full screen, and so, the equivalent sources for these bodies are mostly included in this screen. In Case 3, however, magnetic bodies are distributed widely in full screen, and cannot be replaced by any equivalent source within the screen. This result suggests us that the range of reduction, accordingly the range of observation, should be wide enough compared with the range of interest to get the reduced anomaly.

In addition, the converging speed in the iteration procedure of our method is also improved by around 30%. For instance, Fig.4 displays the root-mean-square difference between two successive approximation of μ in every step for Case 2.

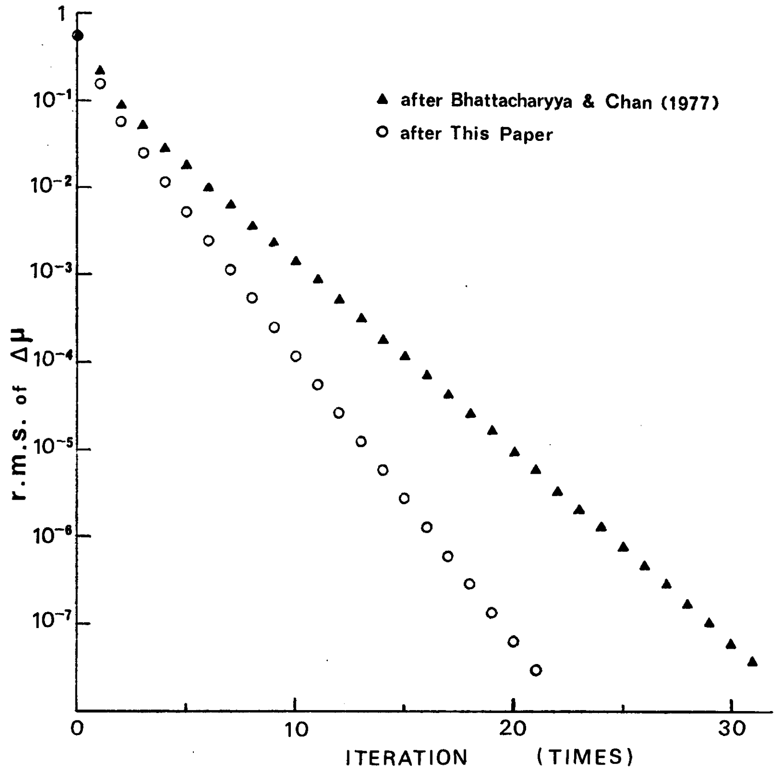

Fig. 4 Convergency of approximation of μ for Case 2 in the iterations. Only the root-mean-square differences between successive approximation of μ are plotted versus iteration time. At *0* iteration the r.m.s. of $\Delta\mu$ is equal to r.m.s. of *0*-th order approximation of μ.

In our theoretical consideration, we have adopted a distribution of vertical magnetic moment as an equivalent source, to avoid approximation. Here it is not essential to adopt "vertical" magnetization, but we may choose any fixed direction of magnetization. However, in equation (15) n should not equal to zero nor so small that the iterating approximation of μ might diverge, and this restricts the shape of observation surface. For example, if we adopt x-direction of magnetization, $(z-\gamma)$ in (13) and $(\gamma'-\gamma)$ in (15) are replaced by $(x-\alpha)$ and $(\alpha'-\alpha)$, respectively, and n denotes the x-component of $\boldsymbol{n}$, where $n'=n(\alpha',\beta',\gamma')$. In this case the observation surface should be monotonous with respect to x-direction. In conclusion, the direction of magnetization other than "vertical" is inconvenient to the practical reduction of magnetic anomaly.

Appendix A

Now we consider a small circular area Q' around the point $Q(\alpha,\beta,\gamma)$ on the surface S. Then the equation (12) yields next expression:

$$T=-\int_{S-Q'}\mu K ds-\int_{Q'}\mu K ds. \qquad \text{(A-1)}$$

If Q' is small enough, we can regard it as a plane, and μ to be constant on it. Then, the second term of the right-hand side of (A-1) can be represented by a double integral in the polar coordinates (r, θ) illustrated in Fig.A. It follows

$$T=T_{Q'}-\int_{S-Q'}\mu K ds, \qquad \text{(A-2)}$$

$$T_{Q'}=-\mu\int_0^{r_0} r dr\int_0^{2\pi} K d\theta, \qquad \text{(A-3)}$$

where r_0 is radius of circular area Q'. Let the observation point $P(x, y, z)$ be on the normal to the surface S at Q. Then, substituting (13) into (A-3), we have

$$T_{Q'}=-\mu\int_0^{r_0} r dr\int_0^{2\pi}\frac{-ln'+r\cos\theta\sqrt{1-n'^2}}{(l^2+r^2)^{3/2}}d\theta \qquad \text{(A-4)}$$

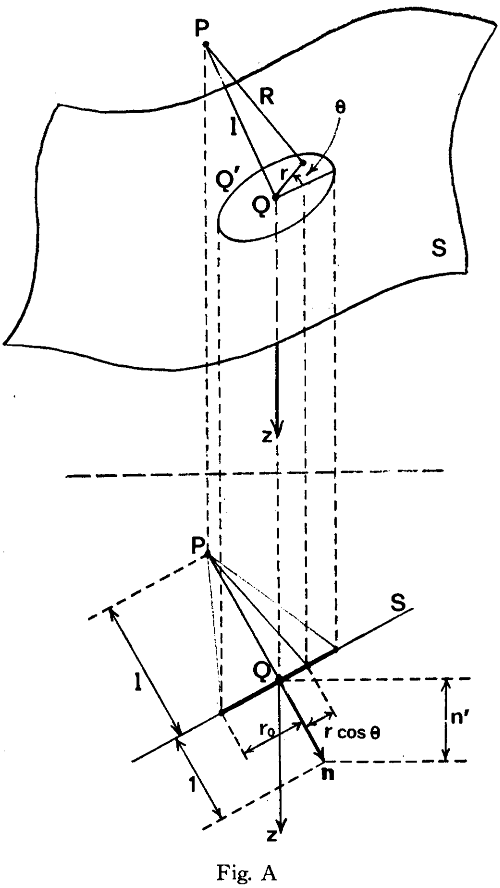

Fig. A

where l is the distance between P and Q, and n' is the z-component of the unit vector $\boldsymbol{n}$ normal to the surface S at Q. Executing the integration over θ and then over r, we obtain

$$\begin{aligned} T_{Q'}&=2\pi\mu ln'\int_0^{r_0}\frac{rdr}{(l^2+r^2)^{3/2}} \\ &=2\pi\mu ln'\left[\frac{-1}{(l^2+r^2)^{1/2}}\right]\Bigg|_{r=0}^{r=r_0} \\ &=2\pi\mu n'\left\{1-\frac{l}{(l^2+r_0^2)^{1/2}}\right\}. \qquad \text{(A-5)}\end{aligned}$$

Therefore, when the observation point P approaches Q along normal to the surface S, l becomes small enough compared with r_0, and in the limiting form we have

$$T_{Q'}=2\pi\mu n'. \qquad \text{(A-6)}$$

This limiting expression is independent of the radius r_0, which should be still small enough. Now we may consider the limit $r_0\to 0$. Accordingly, from (A-2) and (A-6) we obtain

$$T=2\pi\mu n'-\int_{S'}\mu K ds, \qquad \text{(A-7)}$$

where S' is the surface S without Q.

This result is consistent with the formula for the reduction of gravity data presented by BHATTACHARYYA and CHAN (1977).

Appendix B

The analytical formulation of magnetic anomaly T due to an uniformly magnetized rectangular block is given by

$$T(x, y, z)=-J[f]\Big|_{a=a_1}^{a=a_2}\Big|_{b=b_1}^{b=b_2}\Big|_{c=c_1}^{c=c_2}, \qquad \text{(B-1)}$$

$$\begin{aligned} f=&\frac{Mn+mN}{2}\ln\frac{r-a}{r+a}+\frac{Nl+nL}{2}\ln\frac{r-b}{r+b} \\ &+\frac{Lm+lM}{2}\ln\frac{r-c}{r+c}+Ll\tan^{-1}\frac{bc}{ra} \\ &+Mm\tan^{-1}\frac{ca}{rb}+Nn\tan^{-1}\frac{ab}{rc}, \qquad \text{(B-2)}\end{aligned}$$

where $r=\sqrt{a^2+b^2+c^2}$,

$a_1=X_1-x,\ b_1=Y_1-y,\ c_1=Z_1-z,$

$a_2=X_2-x,\ b_2=Y_2-y,\ c_2=Z_2-z.$

Here, (L, M, N) and (l, m, n) are the direction cosines of normal field and magnetization vector, respectively, J is the magnetization intensity, and X_1, X_2, Y_1, Y_2, Z_1, Z_2 are the parameters of the magnetized block, which are indicated in Fig.B.

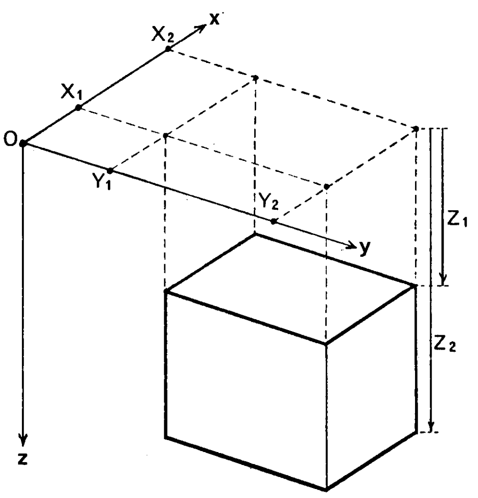

Fig. B

This formulation is derived as follows: The potential $U(x, y, z)$ due to the rectangular block is given by

$$U = J\int_{Z_1}^{Z_2} dz' \int_{Y_1}^{Y_2} dy' \int_{X_1}^{X_2} dx' \cdot \frac{l(x-x')+m(y-y')+n(z-z')}{r^3}, \quad \text{(B-3)}$$

where $r^2=(x-x')^2+(y-y')^2+(z-z')^2$.
Total field anomaly $T(x, y, z)$ is then expressed by

$$T = -L\frac{\partial U}{\partial x} - M\frac{\partial U}{\partial y} - N\frac{\partial U}{\partial z}. \quad \text{(B-4)}$$

Here we put

$$a = x'-x,\ b = y'-y,\ c = z'-z.$$

Then (B-3) becomes

$$U = -J\int_{a_1}^{a_2} da \int_{b_1}^{b_2} db \int_{c_1}^{c_2} dc \frac{la+mb+nc}{r^3}, \quad \text{(B-5)}$$

where $r=\sqrt{a^2+b^2+c^2}$.
Differentiating (B-5) with respect to x, we obtain

$$\frac{\partial U}{\partial x} = J\left[\iint \frac{la+mb+nc}{r^3} db dc\right]\Bigg|_{a_1}^{a_2}\Bigg|_{b_1}^{b_2}\Bigg|_{c_1}^{c_2}$$
$$= J\left[l \tan^{-1}\frac{bc}{ra} + \frac{m}{2}\ln\frac{r-c}{r+c} + \frac{n}{2}\ln\frac{r-b}{r+b}\right]\Bigg|_{a_1}^{a_2}\Bigg|_{b_1}^{b_2}\Bigg|_{c_1}^{c_2}. \quad \text{(B-6)}$$

Substituting (B-6) and similar expressions for $(\partial U/\partial y)$ and $(\partial U/\partial z)$ into (B-4), we have the formulation (B-1) and (B-2).

Here (B-2) can be alternated by some other expressions, for example, f may be expressed by

$$f = -(Mn+mN)\ln(r+a) - (Nl + nL)\ln(r+b) - (Lm+lM)\ln(r+c) - Ll\tan^{-1}\frac{ra}{bc} - Mm\tan^{-1}\frac{rb}{ca} - Nn\tan^{-1}\frac{rc}{ab}$$

Either expression for f should be given modified formula in some cases such as $a=0$, $b=0$, and/or $c=0$. In practical calculations at discrete points, however, we can get sufficiently approximated values from equation (B-2) or some other alternatives, regarding zero-value as if it is a very small non-zero value.

REFERENCES

1) BHATTACHARYYA, B.K. and K.C. CHAN (1977): Reduction of Magnetic and Gravity Data on an Arbitrary Surface Acquired in a Region of High Topographic Relief, *Geophysics*, vol.42, 1411-1430.

2) DAMPNEY, C.N.G. (1969): The Equivalent Source Technique, *Geophysics*, vol.34, 39-53.

3) HENDERSON, R.G. and L. CORDELL (1971): Reduction of Unevenly Spaced Potential Field Data to a Horizontal Plane by Means of Finite Harmonic Series, *Geophysics*, vol.36, 856-866.

4) SYBERG, F.J.R. (1972): Potential Field Continuation between General Surfaces, *Geophys. Prosp.*, vol.20, 267-282.

要 旨

任意曲面上で測定された磁気異常のリダクション

中 塚 正

不規則な曲面上で測定された磁気異常を別の曲面上での値に Reduce する方法については，古くからフーリェ解析に基づく方法が研究されてきたが，BHATTACHARYYA and CHAN (1977) は測定面そのものの上に等価モデルをもってくるという卓抜したアイデアを導入して，その解法を示した。彼等の等価モデルは曲面に垂直な磁化の分布であるが，その理論展開の中に誤りがあり，結果的に彼等の方法は，測定面の曲率が充分小さいという近似の下にのみ有効であることがわかった。こうした不合理な近似を取り除くため，本論文では曲面の形にかかわらず一定方向（ここでは鉛直方向を扱っている）の磁化分布を等価モデルとして採用し，その理論式を厳密に展開した。また，この方法と BHATTACHARYYA and CHAN (1977) の方法との比較をモデルケースについて行ない，リダクション結果が改善されることを示した。Fig. 1の例では測定面の形がおだやかで両者の結果に大きな差異はないが，Fig. 2の例および Fig. 3の中央部分では顕著な差が見られ，本論文の方法の優位を示している。これらの例における測定面の形状は，地上磁気探査の場合には現実にあり得る程度のものである。Fig. 3の縁辺部ではいずれの結果にも，解析的に求めたものとかなりの差異が見られるが，これは数値計算において無限曲面上での積分を有限区間で打切った効果によるものであり，こうしたリダクションは結果を得たい範囲に較べて充分広い範囲のデータに対して行なうことが必要である。